RESEARCH ARTICLE

Association Between Cytoplasmic CRABP2, Altered Retinoic Acid Signaling, and Poor Prognosis in Glioblastoma

Rong-Zong Liu,[1] Shuai Li,[1] Elizabeth Garcia,[1] Darryl D. Glubrecht,[1] Ho Yin Poon,[1] Jacob C. Easaw,[2] and Roseline Godbout[1]

ABSTRACT: Retinoic acid (RA), a metabolite of vitamin A, is required for the regulation of growth and development. Aberrant expression of molecules involved in RA signaling has been reported in various cancer types including glioblastoma multiforme (GBM). Cellular retinoic acid-binding protein 2 (CRABP2) has previously been shown to play a key role in the transport of RA to retinoic acid receptors (RARs) to activate their transcription regulatory activity. Here, we demonstrate that CRABP2 is predominantly located in the cytoplasm of GBM tumors. Cytoplasmic, but not nuclear, CRABP2 levels in GBM tumors are associated with poor patient survival. Treatment of malignant glioma cell lines with RA results in a dose-dependent increase in accumulation of CRABP2 in the cytoplasm. CRABP2 knockdown reduces proliferation rates of malignant glioma cells, and enhances RA-induced RAR activation. Levels of CRYAB, a small heat shock protein with anti-apoptotic activity, and GFAP, an astrocyte-specific intermediate filament protein, are greatly reduced in CRABP2-depleted cells. Restoration of CRYAB expression partially but significantly reversed the effect of CRABP2 depletion on RAR activation. Our combined *in vivo* and *in vitro* data indicate that: (i) CRABP2 is an important determinant of clinical outcome in GBM patients, and (ii) the mechanism of action of CRABP2 in GBM involves sequestration of RA in the cytoplasm and activation of an anti-apoptotic pathway, thereby enhancing proliferation and preventing RA-mediated cell death and differentiation. We propose that reducing CRABP2 levels may enhance the therapeutic index of RA in GBM patients.

GLIA 2016;64:963–976

Key words: brain tumor, retinoic acid receptor, retinoic acid resistance, alpha-crystallin B

Introduction

Astrocytomas are the most common brain malignancies, accounting for ~75% of all primary gliomas (Ostrom et al., 2015). The World Health Organization (WHO) grading system classifies astrocytomas as Grades I to IV. Grade IV astrocytoma (also known as glioblastoma multiforme or GBM), makes up 73.5% of all astrocytomas (Ostrom et al., 2015) and is the most aggressive of all primary brain tumors with a median survival of 12–15 months (Johnson and O'Neill, 2012). Because of their highly infiltrative nature, GBM tumors invariably recur after initial surgery, radiation therapy and chemotherapy. GBM tumors are characterized by extensive heterogeneity at the cellular and molecular levels (Sottoriva et al., 2013), which poses a major challenge to the design of effective therapies. To this day, there is no curative intervention for GBM despite decades of intense research effort.

Retinoic acid (RA) is an essential signaling molecule that regulates multiple biological processes, including cell proliferation, differentiation, and death (Duester, 2008; Gudas, 1994; Means and Gudas, 1995; Napoli, 1996; Noy, 2010). RA has long been believed to hold great promise for cancer chemoprevention and chemotherapy, as: (i) *in vitro* studies have shown that RA and its derivatives, collectively called retinoids, inhibit growth and induce apoptosis in a variety of epithelial cancer cells (Gudas, 1992; Lotan, 1996; Mongan and Gudas, 2007; Tanaka and De Luca, 2009), (ii) undifferentiated stem-like cells, thought to underlie tumor self-renewal and resistance to therapeutic agents, appear to be particularly susceptible to the

View this article online at wileyonlinelibrary.com. DOI: 10.1002/glia.22976

Published online February 19, 2016 in Wiley Online Library (wileyonlinelibrary.com). Received July 31, 2015, Accepted for publication Jan 25, 2016.

Address correspondence to Roseline Godbout, Department of Oncology, Cross Cancer Institute, 11560 University Avenue, Edmonton, Alberta, Canada T6G 1Z2, E-mail: rgodbout@ualberta.ca

From the [1]Department of Oncology, University of Alberta, Cross Cancer Institute, 11560 University Avenue, Edmonton, Alberta, T6G 1Z2, Canada; [2]Division of Medical Oncology, University of Calgary, Calgary, Alberta, T2N 4N2, Canada

Additional Supporting Information may be found in the online version of this article.

© 2016 Wiley Periodicals, Inc.

differentiation properties of retinoids (Campos et al., 2010; Gudas and Wagner, 2011), and (iii) retinoids have been successfully used in the treatment of acute promyelocytic leukemia (APL) (Huang et al., 1988; Petrie et al., 2009; Warrell et al., 1991). However, clinical trials to test the efficacy of retinoids for the treatment of solid cancers have for the most part produced disappointing results due to toxic side effects and development of RA resistance (Boorjian et al., 2007; Recchia et al., 2001; Shin et al., 2002; Singletary et al., 2002). Notably, rather than inhibit growth, RA treatment has been shown to enhance proliferation in some cancers (Garattini et al., 2007; Schug et al., 2007; Verma et al., 1982).

Over the last 20 years, significant progress has been made in our understanding of the mechanisms of action of RA. As RA is hydrophobic, its cellular trafficking is facilitated by binding to members of the intracellular lipid-binding protein (iLBP) family, known as cellular retinoic acid-binding protein 1 (CRABP1) and 2 (CRABP2) (Donovan et al., 1995), and fatty acid binding protein 5 (FABP5) (Tan et al., 2002). Once bound by these proteins, RA is transported to different parts of the cell to either actualize its biological effects or be metabolized (Budhu and Noy, 2002; Chambon, 1996; Dong et al., 1999; Fiorella and Napoli, 1994; Napoli, 1996). Alternatively, RA can be sequestered in the cytoplasm when bound to its binding proteins, thereby modulating RA's bioavailability and toxicity (Fiorella and Napoli, 1994; Napoli, 1996). A key component of RA action is its mobilization to the nucleus where it then acts as an activator of nuclear receptors that in turn regulate the transcription of target genes involved in growth, development and differentiation (Budhu and Noy, 2002; Dong et al., 1999). All-trans-RA (ATRA, RA) activates retinoic acid receptors (RARα, RARβ, RARγ), whereas 9-cis-RA activates RARs as well as retinoid-X-receptors (RXRα, RXRβ, RXRγ) (Chambon, 1996; Mangelsdorf, 1994). RARs usually heterodimerize with RXRs, with the dimer functioning as a transcription factor. Peroxisome proliferator-activated receptor PPARβ is another nuclear receptor that can be activated by RA, an interaction that is mediated by nuclear FABP5 bound to RA (Schug et al., 2007; Tan et al., 2002).

Impaired RA signalling is frequently observed in human cancers including GBM (Campos et al., 2011, 2015; Esteller et al., 2002; Williams et al., 2009). GBM cells are extremely resistant to RA action and it has been postulated that down-regulation of CRABP2, the intracellular RA-transporter, and ALDH1A1, the RA-synthesizing enzyme, are factors contributing to RA resistance in GBM cells (Adam et al., 2012; Campos et al., 2011, 2015). Here, we show that CRABP2, normally associated with RA nuclear signaling, preferentially localizes to the cytoplasm of GBM tumor cells and is associated with a poor patient prognosis. Importantly, RA treatment of CRABP2-expressing malignant glioma cells results in cytoplasmic accumulation of CRABP2, and CRABP2 depletion is accompanied by decreased cell proliferation and increased activation of RAR receptors in RA-treated cells.

Materials and Methods

Glioblastoma Tissue Microarray (TMA) Immunohistochemistry

GBM tumor tissues were collected from patients diagnosed and centrally reviewed in a single institution. Ethical approval was obtained according to institutional guidelines (2006, Tom Baker Cancer Center, Calgary, Canada). Tumor tissues were fixed in formalin and embedded in paraffin. A detailed description of additional clinical data corresponding to the TMA samples is provided in Supporting Information Table 1.

The sources or references for the malignant glioma (MG) cell lines used in this study are: T98, from Walter Nelson-Rees, Naval Biomedical Research Station, Oakland, CA; U87, U251, and U373, from Jorgen Fogh, Sloane Kettering Institute, Rye, NY; A172, from Stuart A. Aaronson, NCI, Bethesda, MD; CLA, from Paul Kornblith, Albert Einstein College of Medicine, Montefiore Medical Center, Bronx, NY). M016, M021, M049, and M103 have been previously described (Brun et al., 2009; Godbout et al., 1992, 1998). Cells were cultured at 37°C in a 5% CO_2 atmosphere in Dulbecco's Modified Eagle's Medium (DMEM) supplemented with 10% fetal bovine serum (FBS) and penicillin and streptomycin.

The TMA consists of at least 3 cores from each primary GBM tumor. TMA slides were deparaffinized in xylene, rehydrated and microwaved for 20 min in epitope retrieval buffer (10 mM citrate, 0.05% Tween-20 with pH 6.0). TMAs were then immunostained with anti-CRABP2 antibody (1:200; ProteinTech Group, Inc.; Cat. # 10225-1-AP) and the signal was detected using DakoCytomationEnVision+ anti-rabbit secondary system (Dako, CA). Tissues were counterstained with hematoxylin. All samples were independently evaluated by two observers (DDG and RZL) blinded to clinical outcomes. Cytoplasmic and nuclear CRABP2 immunoreactivity were separately evaluated based on average staining intensity and percent of cells stained throughout the tumor tissue. Staining intensity was scored on a scale of 0 (negative), 1 (weak), 2 (intermediate) and 3 (strong). For cytoplasmic CRABP2, a tumor tissue with more than 50% cells (averaged over the three cores) showing signal intensity score 2 and/or 3 was classified as "high" expression, otherwise as "low" expression. For nuclear CRABP2, a tumor tissue with more than 25% of cells showing an intensity score of 1, 2, and/or 3 was identified as "positive", otherwise "negative". Scores obtained from the two independent TMA evaluators were in good ($K = 0.79$) and very good ($K = 0.86$) agreement for CRABP2 cytoplasmic and nuclear immunoreactivity, respectively, based on Cohen's inter-rater agreement test.

siRNA Transfection

The human MG cell line U251 was transfected with 10 nM of the following Stealth siRNAs (Invitrogen) targeting distinct regions of the CRABP2 mRNA (siRNA1: 5'-UGGUCUGUGAGCAGAAGCUCC UGAA-3'; siRNA2: 5'-UGGACCAGAGAACUGACCAACGAUG-3', siRNA3: 5'-GGGUGAAUGUGAUGCUGAGGAAGAU-3', siRNA4:

5'-GCGCACCACAGAGAUUAACUUCAAG-3') or 10 nM control siRNA with low or moderate GC content using RNAi-MAX Lipofectamine reagent (Invitrogen). After 16 − 18 h, the medium was replaced with DMEM containing 10% FCS and the cells cultured for an additional 48 h before harvest or subsequent experiments.

Western Blotting

Western blot analysis was carried out using 40 μg whole cell or cytoplasmic extracts or 20 μg nuclear extracts per lane. Proteins were separated by SDS-PAGE and electroblotted onto nitrocellulose membranes. Blots were immunostained with primary antibodies against CRABP2 (1:1,000; ProteinTech Group, Inc.; Cat. # 10225-1-AP), p53 (1:1,000; Santa Cruz Biotechnology; Cat. # sc-126), RARα (1:500; Santa Cruz Biotechnology; Cat. # sc-551), RARβ (1:500; Santa Cruz Biotechnology; Cat. # sc-552), cyclin E (1:500, BD Pharmingen; Cat. # 554182), CRYAB (1:1,000; Enzo Life Sciences; Cat. # ADI-SPA-222), GFAP (1 : 500; BD Pharmingen; Cat. # 556330), β-actin (1:100,000; Sigma; Cat. # A3854), α-tubulin (1:10,000; DSHB; Cat. # 12G10), lamin A/C (1:1,000; Thermo Fisher Scientific; Cat. # MA3-1000) and FABP7 (1:1,000) (Godbout et al., 1998). Primary antibodies were detected with horseradish peroxidase-conjugated secondary antibodies and visualized using the ECL detection system (GE healthcare) or the Immobilon Western detection system (Millipore, Billerica, MA).

RT-PCR

Total RNA was isolated from human MG cell lines using TRIzol reagent (Invitrogen). First strand cDNAs were synthesized using SuperScript II reverse transcriptase (Invitrogen) according to the protocol provided by manufacturer. The following oligonucleotide primers were used for PCR amplification: *CRABP2*, sense 5'-TGCT GAGGAAGATTGCTGTG-3', antisense 5'- TCTTTGTTGGTGT AGGGGAG-3; *CRYAB*, sense 5'-CTTCGGAGAGCACCTGTTG-3', antisense 5'-TTCACGGGTGATGGGAATG-3'; *GFAP*, sense 5'-TCAAGAGGAACATCGTGGTG −3', antisense 5'-AGGAATCAG GGATGTGGAG-3'; β-actin, sense 5'-CTGGCACCACACCTTC TAC-3', antisense 5'-CATACTCCTGCTTGCTGATC-3'. PCR reactions and agarose gel electrophoresis were carried out as previously described (Liu et al., 2011).

Cell Proliferation and Cell Cycle Progression Analysis

After siRNA depletion, U251 cells were seeded in 12-well plates at 10,000 cells per well. Cells from triplicate wells were counted at the indicated time points with a Coulter Particle and Size Analyzer (Coulter Corporation). Cell counts were averaged and differences were analyzed with the two-sided student's *t*-test. The MTS cell proliferation assay was carried out using the CellTiter 96 Aqueous Non-Radioactive Cell Proliferation Assay kit (Promega). Three thousand cells were seeded in each well (5 duplicate wells per treatment) of a 96-well plate and cultured in DMEM supplemented with 10% FBS for 72 h after siRNA knockdown. Cell viability was measured based on absorbance as per the manufacturer's protocol. For cell cycle analysis, cells were transfected with either scrambled or CRABP2 siRNAs and cultured in DMEM medium supplemented with 10% FBS. Subconfluent cells were harvested by trypsinization and fixed in ice-cold 70% ethanol for 2 h. Cells were then incubated in a propidium iodide (PI, SIGMA) staining buffer (1X PBS containing 3.8 mM sodium citrate, 50 μg/mL PI and 100 μg/mL RNase A) at 4°C for 3 h. Cell cycle distribution was analyzed by flow cytometry using the FACSCanto II system (BD Biosciences). Three independent experiments were carried out using CRABP2 siRNA1 and 2, with two additional siRNAs (3 and 4) used to confirm the data obtained with siRNAs 1 and 2. Each experiment was performed using triplicate plates for each siRNA.

Luciferase Reporter Analysis

Following CRABP2 depletion with siRNA, U251 or M049 MG cells were seeded in 12-well plates and cultured in DMEM supplemented with 10% FBS for 24 h, and each well transfected with 0.5 μg plasmid DNA (pGL3-RARE-luciferase) harboring a luciferase reporter gene driven by a retinoic acid receptor response element (RARE; Addgene) using polyethyleneimine (PEI; Polysciences). To test overexpression of CRABP2 on RAR activation, T98 MG cells were co-transfected with pGL3-RARE-luciferase and pcDNA3-CRABP2. Cells were cultured in transfection medium overnight, at which time the medium was replaced and cells cultured for an additional 24 h. For RA treatment, cells were cultured in serum-free medium in the absence or presence of RA for 6 h. Cell lysates were prepared using the 1X Luciferase Cell Lysis Reagent (Promega) and luciferase activity was measured using the Luciferase Assay System (Promega) and quantitated using a FLUOstar OPTIMA microplate reader (BMG Labtech) following the manufacturer's instructions. Each experiment was carried out in triplicate, with readings averaged for each experiment.

Statistical Analysis

All statistical analyses were performed using MedCalc version 12.4.0.0 (MedCalc Software). The two-sided student *t*-test was employed to compute the significance level of the difference in: (i) cell growth rates, (ii) luciferase activity among control and RA-treated cells and control and CRABP2-depleted cells, and (iii) percentage of cell counts in specified cell cycle phases. Recurrence-free survival curves were generated by the Kaplan-Meier method and the survival probabilities between patient groups with high/positive or low/negative subcellular CRABP2 immunoreactivity or RNA levels were compared by logrank test. Receiver operating characteristic (ROC) curve analysis was employed to determine the cut-off point of mRNA levels (*z*-scores) of CRABP2 for overall and disease-free survival analysis. The significance of the association between *CRYAB* and *GFAP* RNA levels was tested with Pearson's correlation analysis.

Results

Aberrant Subcellular Distribution of CRABP2 in GBM Tissues and Its Association with Clinical Outcomes

As an intracellular chaperone for RA, CRABP2 can be found in both the cytoplasm and nucleus. In the presence of RA, CRABP2 translocates to the nucleus, where it interacts with RAR thereby activating its transcription regulation activity. However, CRABP2 can also be retained in the cytoplasm where

it sequesters RA, or, as shown by recent studies, where it interacts with the RNA-binding and stabilizing protein HuR to control RNA stability (Vreeland et al., 2014a,b). To this day, the cytoplasmic roles of CRABP2 remain poorly understood.

To examine the subcellular distribution of CRABP2 in GBM, we immunostained a tissue microarray consisting of 116 human GBM tumor tissues with an antibody that specifically recognizes CRABP2 (Liu et al., 2015). Immunoreactivity data from 103 GBM tissues were of sufficient quality to allow scoring: 0 (negative), 1 (weak), 2 (moderate) and 3 (strong). Of the 103 GBM tissues, 86 (83.5%) tumors were positive for cytoplasmic CRABP2, with scores of 1 to 3. However, only 25 (24.3%) tumors were positive for nuclear CRABP2 (Fig. 1A,B). Moderate to strong immunostaining (scores of 2 to 3) was observed in the cytoplasm of 28/86 (32.6%) GBM tissues (or 27.2% of 103 GBM tissues) and in the nucleus of 7/25 (28%) (or 6.8% of 103 GBM tissues). CRABP2 was detected exclusively in the cytoplasm of sixty-two tumors, and exclusively in the nucleus in only one tumor. These data indicate that CRABP2 is predominantly cytoplasmic in GBM tumors.

To determine the potential effect of subcellular CRABP2 levels on patient prognosis, we performed Kaplan-Meier univariate survival analysis of the GBM patient cohort with 5 years of clinical follow-up data. To this end, we divided the patient cohort into subpopulations with high (moderate to strong immunoreactivity; $n = 28$) and low (weak or negative immunoreactivity; $n = 75$) cytoplasmic CRABP2 levels, or subpopulations with positive ($n = 25$) and negative ($n = 78$) nuclear CRABP2 levels. Patients with high cytoplasmic CRABP2 levels had significantly lower recurrence-free survival probability compared to those with low cytoplasmic levels ($P = 0.01$; Fig. 1C, left panel). In contrast, nuclear CRABP2 levels had no effect on recurrence-free survival ($P = 0.98$; Fig. 1C, right panel). Neither cytoplasmic nor nuclear CRABP2 levels showed significant prognostic value on overall survival for GBM patients (data not shown).

Next, we tested the impact of *CRABP2* RNA levels on clinical outcomes using a 401 GBM patient TCGA microarray dataset (with recorded recurrence/progression and vital status) (Brennan et al., 2013) retrieved from cBioportal for Cancer Genomics (Cerami et al., 2012; Gao et al., 2013) on November 2015. Elevated *CRABP2* RNA levels were significantly associated with poorer overall (HR = 1.88, $P < 0.01$; left panel) and disease free prognosis (HR = 2.42, $P < 0.05$; right panel) (Fig. 1D) within 24 months of follow-up time. These results suggest that CRABP2 levels in GBM tumors may represent a risk factor for early recurrence and death, and that the adverse effect of elevated CRABP2 levels may be attributed to the aberrant accumulation of CRABP2 in the cytoplasm of GBM cells.

CRABP2 Knockdown Represses Cell Growth in U251 Cells

One of the major biological activities of RA is to induce inhibition of cell growth by binding and activating RARs in the nucleus, a function that is mediated by CRABP2. To determine whether CRABP2 is expressed in MG cell lines (i.e., cell lines derived from high grade astrocytomas), we carried out western blot analysis of 10 MG cell lines. CRABP2 was easily detected in 5 cell lines (M021, U87, M049, M103, U251) and barely detectable in one cell line (U373) (Fig. 2A).

To study the effect of CRABP2 levels on cell proliferation, we transfected U251 cells with siRNAs that specifically target CRABP2. CRABP2 knockdown was confirmed by both RT-PCR and western blot analysis (>90%; Fig. 2B,C). We used cell counts to measure the growth rate of control and CRABP2-depleted U251 cells. The growth rate of CRABP2-depleted cells was significantly reduced compared to cells transfected with scrambled siRNAs (Figure 2D). The difference between the two cell populations was statistically significant starting from 96 h in culture ($P < 0.01$). The experiment was repeated using a second siRNA targeting a distinct region of the CRABP2 mRNA, with similar results (data not shown). To confirm the anti-proliferative effect of CRABP2 depletion, we measured cell proliferation in control and CRABP2-depleted cells using the MTS Cell Proliferation Assay system, a colorimetric-based assay for the quantification of live cells. Compared to control siRNA, depletion of CRABP2 with siRNA1 or siRNA2 resulted in 35% and 62% reduction, respectively, in absorbance (OD_{490}). These results indicate that CRABP2 may play a role in enhancing cell proliferation/survival in GBM cells.

To explore the mechanism by which CRABP2 promotes cell growth, we examined the changes in cell cycle progression in control versus CRABP2-depleted U251 cells. Four siRNAs targeting distinct regions of CRABP2 were used for this experiment. We observed >90% reduction in CRABP2 protein levels in U251 cells transfected with each of the four CRABP2 siRNAs relative to scrambled siRNA control (Fig. 3A). CRABP2 knockdown resulted in changes in the cell cycle distribution, with a significant reduction in G1-phase cells (72.6% for control cells vs an average of 54.3% for CRABP2-depleted cells) and a significant increase in S-phase (9.8% vs. 21.2%) and G2-phase (16% vs. 23.5%) cells (Fig. 3B–G). These data suggest that CRABP2 promotes G1/S transition in U251 cells, resulting in a more rapid progression through the cell cycle.

CRABP2 Accumulates in the Cytoplasm of MG Cells in Response to RA Treatment

As discussed earlier, the subcellular distribution of CRABP2 in response to RA is believed to be a key factor in cellular response to RA. To this end, we treated both U251 and M049 MG cell lines with increasing amounts of all-trans RA and then prepared

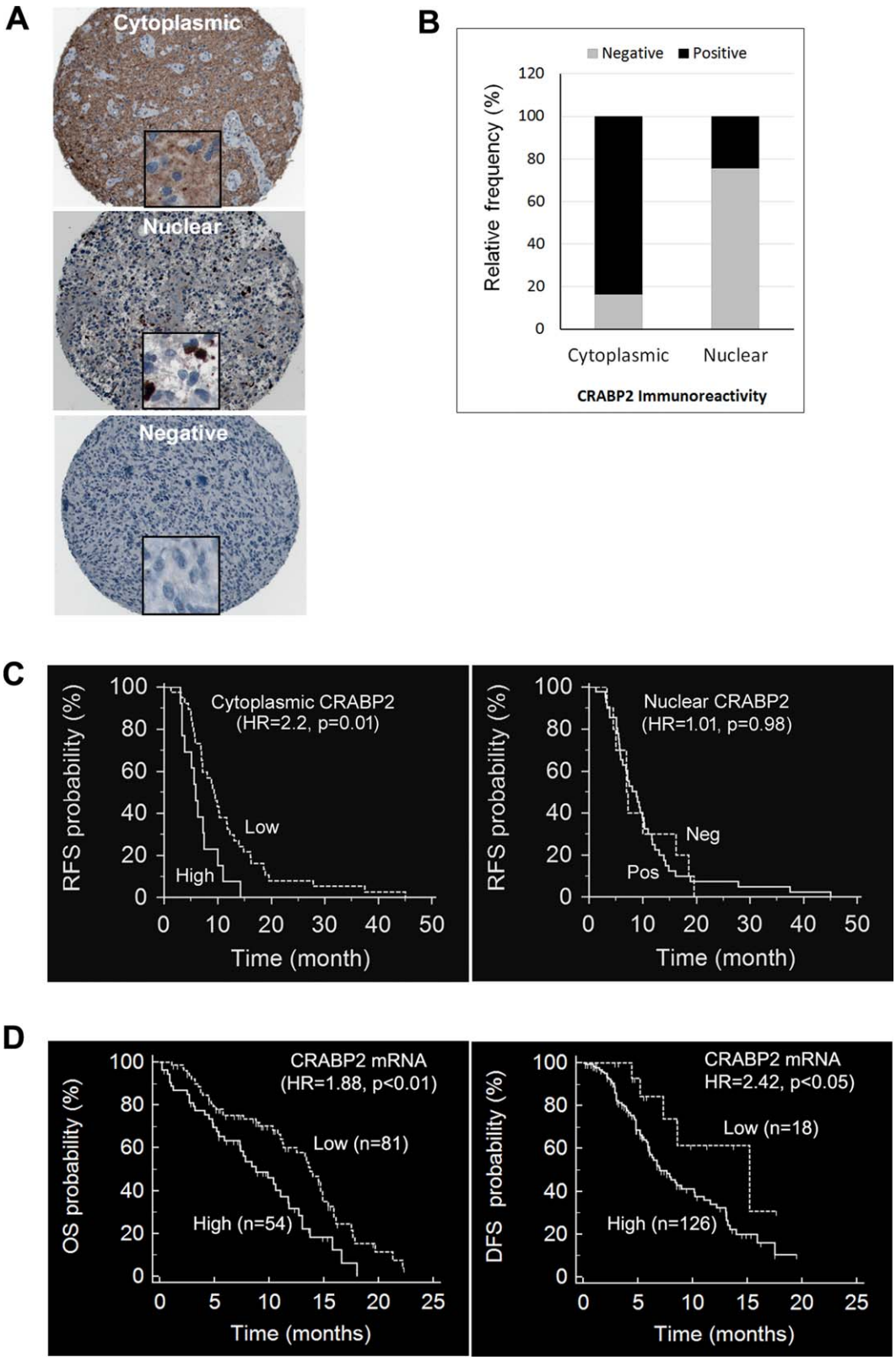

FIGURE 1: Association of CRABP2 levels and subcellular distribution with clinical outcomes in GBM. (A-C) CRABP2 immunohistochemical scores were obtained by immunostaining a tissue microarray prepared from 103 GBM patients. (A) Selected TMA sections showing cytoplasmic, nuclear or negative CRABP2 immunostaining. A magnified region from each image is shown in the box. (B) Relative frequency of tumors showing negative or positive CRABP2 immunostaining in the cytoplasm or nucleus. (C) Recurrence-free survival (RFS) probability based on cytoplasmic (left) and nuclear (right) immunostaining scores from the 103-patient GBM cohort. The patient population was divided into high and low immunoreactivity for cytoplasmic CRABP2, or positive (Pos) and negative (Neg) immunoreactivity for nuclear CRABP2, as defined in Materials and Methods. (D) Overall (OS; left) and disease-free (DFS; right) survival curves were generated with low or high *CRABP2* RNA levels in GBM tumor tissues obtained from a TCGA dataset (Brennan et al., 2013) deposited in cBioportal network (Cerami et al., 2012; Gao et al., 2013). The hazard ratio (HR) and statistical significance level (p) are indicated. "n" indicates sample size. [Color figure can be viewed in the online issue, which is available at wileyonlinelibrary.com.]

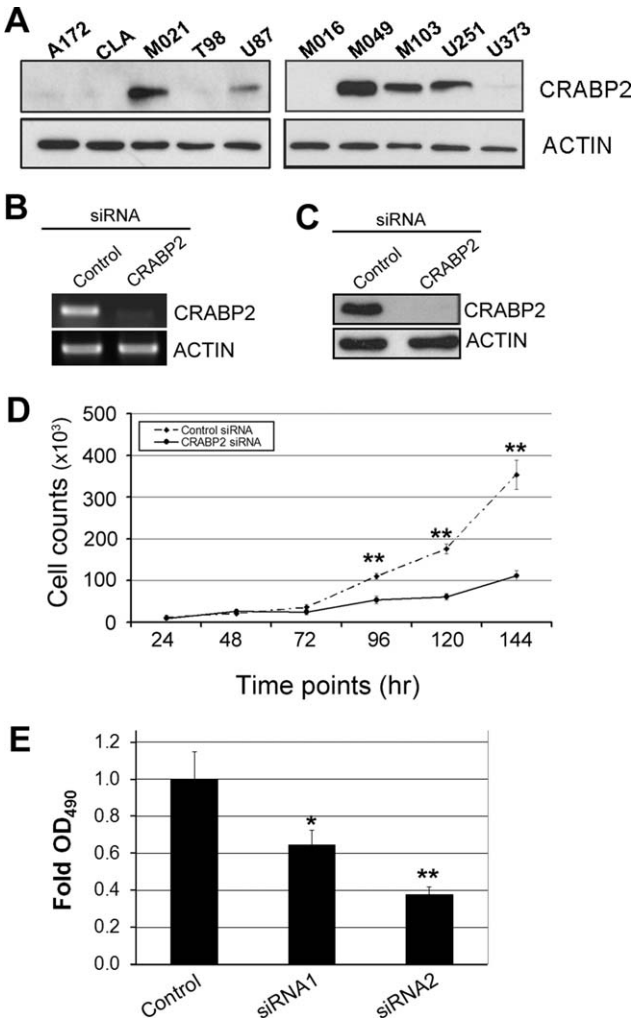

FIGURE 2: CRABP2 affects the growth rate of U251 MG cells. (A) Western blot analysis of whole cell lysates prepared from ten MG cell lines using anti- CRABP2 and anti-β-actin (loading control) antibodies. (B) RT-PCR analysis showing >80% reduction in *CRABP2* RNA levels in U251 cells transfected with CRABP2 siRNA. (C) Western blot analysis showing >80% depletion of CRABP2 protein in U251 cells transfected with CRABP2 siRNA. (D) Growth rate curves of U251 cells transfected with control or CRABP2 siRNA. Cells were seeded in 12-well plates at 10,000 cells per well and cultured in DMEM supplemented with 10% FBS until harvested and counted at the indicated time points. The results of one experiment is shown in (D), with similar data obtained in one additional experiment. (E) The MTS assay was used to confirm the effect of CRABP2 depletion on cell proliferation. Both CRABP2 siRNA1 and 2 were included in this analysis. "*" denotes $p < 0.05$; "" $p < 0.01$.**

cytoplasmic and nuclear extracts from control and RA-treated cells. CRABP2 was preferentially located in the cytoplasm of both U251 and M049 cells in the absence of RA (Fig. 4A,B). An increase in cytoplasmic CRABP2 levels was observed in cells treated with RA (Fig. 4A,B).

Next, we used immunofluorescence to examine the subcellular distribution of CRABP2 in U251 cells upon RA treatment. In cells growing in medium without RA, we observed CRABP2 throughout the cell with a stronger signal in the cytoplasm compared to nucleus. When cells were treated with 5 μM of RA, we observed a marked increase in CRABP2 immunoreactivity in the cytoplasm but not in the nucleus (Fig. 4C). These results indicate that CRABP2 levels are induced by RA in MG cells; however, CRABP2 does not translocate to the nucleus in the presence of RA.

CRABP2 Attenuates RA-Induced RAR Activation

To address whether CRABP2 affects RA signaling to RARs in MG cells, we examined the transcriptional activity of RAR using the luciferase reporter gene driven by an RAR element (RARE). We first measured luciferase activity in U251 cells transfected with scrambled or CRABP2 siRNAs in the absence or presence of RA. There was little change (~1.2-fold increase) in luciferase activity in cells transfected with CRABP2 siRNA compared to scrambled siRNA in the absence of RA. However, in cells transfected with control siRNA, luciferase activity (a measure of RAR activation) increased ~4-fold in the presence of RA (0.5 − 5 μM) compared to cells cultured in RA-free medium. Moreover, luciferase activity more than doubled in CRABP2-depleted cells in the presence of RA (~7- to 10-fold increase in luciferase activity compared to the 4-fold increase observed in control cells) (Fig. 5A). To eliminate the possibility of siRNA off-target effects, we repeated the transfection using a second CRABP2 siRNA targeting a different region of the *CRABP2* mRNA. Similar results were obtained; i.e., CRABP2 depletion significantly increased RA-induced RAR transcriptional activity compared to control cells (Fig. 5B).

To ensure that the observed effect of CRABP2 on RA signaling through RAR was not cell line-specific, we repeated the experiment in a second MG cell line that expresses CRABP2, M049. Of note, M049 expresses the highest CRABP2 levels of all 10 MG lines tested. Transfections were carried out as detailed for U251. In contrast to U251, we observed a significant induction in RAR activation (~5-fold increase) upon CRABP2 depletion in the absence of RA (Fig. 5C). The level of RAR induction in control cells in the presence of RA was similar to that of U251 (4- to 5-fold increase). However, a much higher increase in luciferase activity, 45- to 46-fold, was observed in CRABP2-depleted M049 cells in the presence of RA (Fig. 5C). These results indicate that CRABP2 plays a negative role in RAR activation in the presence of RA.

Next, we used a gain-of-function approach to address the inhibitory effect of CRABP2 on RAR activity. We co-transfected the CRABP2-negative T98 MG cell line with the RARE-driven luciferase reporter gene along with a CRABP2 expression construct (pcDNA3 carrying full-length CRABP2 cDNA). RA treatment (0.5 − 5 μM) resulted in a 2.5- to 2.7-fold increase in luciferase activity in T98 cells transfected with empty vector. Ectopic expression of CRABP2 resulted in significantly reduced

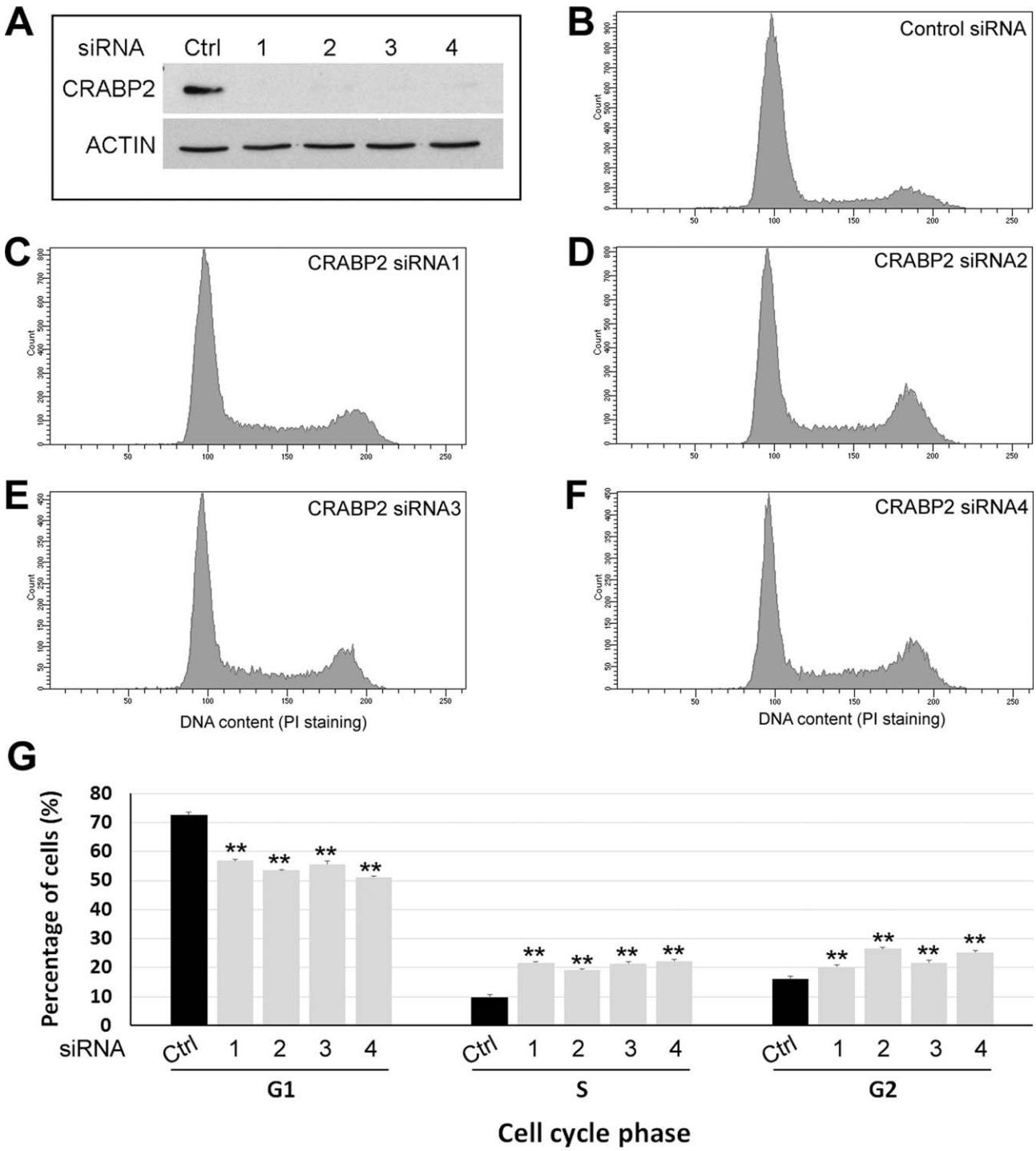

FIGURE 3: Effect of CRABP2 depletion on the cell cycle. U251 cells were transfected with scrambled (control) siRNAs or CRABP2 siRNAs. (A) Western blot analysis shows a significant decrease in CRABP2 levels (>90%) in CRABP2-depleted (labeled 1-4) compared to control (Ctrl) cells. (B-F) Representative images of the cell cycle distribution of cells transfected with scrambled (control) or CRABP2 siRNAs. (G) Histograms showing the average percentage of cells in the G1, S and G2 phases of the cell cycle in control versus CRABP2-depleted cells. The values shown in individual columns represent the arithmetic mean of cell counts from triplicate wells transfected with the same siRNA. The two-sided student t-test was used to analyze the significance of differences in cell count percentages in the G1, S and G2 phases of the cell cycle between control and CRABP2-depleted cells [Ctrl, black columns; CRABP2-depleted (1-4), gray columns]. Standard deviation is indicated by the error bars. Three independent experiments were carried out with CRABP2 siRNA1 and 2. The data were confirmed using CRABP2 siRNA3 and 4. ** denotes $p < 0.01$.

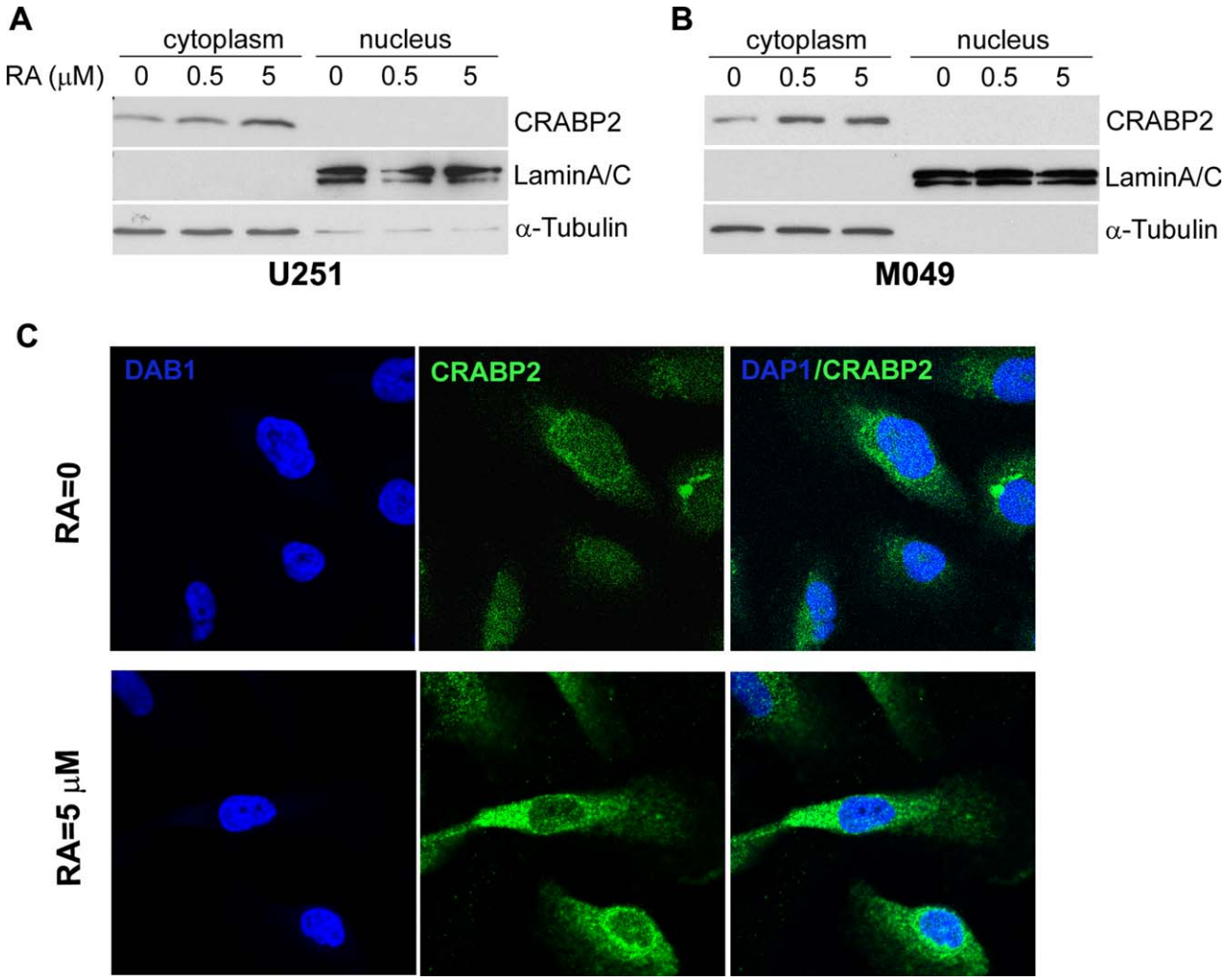

FIGURE 4: CRABP2 accumulates in the cytoplasm of MG cells in the presence of retinoic acid. (A-B) Immunodetection of CRABP2 in the cytoplasm and nucleus of U251 and M049 cells treated with increasing amounts of RA as indicated. Human lamin A/C and α-tubulin were used as loading controls for nuclear and cytoplasmic extracts, respectively. (C) Confocal microscopy images of U251 cells immunostained with anti-CRABP2 followed by donkey anti-rabbit Cy5 secondary antibodies (green) in the absence (RA = 0) or presence (RA = 5 μM) of RA. Nuclear DNA was stained with 4′6-diamiddino-2-phenylindole (DAPI, blue). [Color figure can be viewed in the online issue, which is available at wileyonlinelibrary.com.]

luciferase activity in the absence of RA (~40%), with even greater reduction in the presence of RA (~70%) compared to control cells cultured in the absence of RA (Fig. 5D). These combined results indicate that CRABP2 plays an inhibitory role in RA-induced RAR activation in MG cells.

CRABP2 Affects Molecular Pathways Involved in Cell Cycle Progression and Apoptosis Resistance

To further investigate the mechanism underlying CRABP2/RA-mediated effects on cell growth and RAR activation, we examined proteins implicated in cellular response to RA and/or MG growth. As expected, we found CRABP2 to be induced by RA in a dose-dependent manner in U251 control cells. CRABP2 was barely detected in cells transfected with CRABP2 siRNA regardless of RA treatment (Fig. 6A). We observed an approximately two-fold increase in p53 levels in both control and CRABP2-depleted cells treated with RA, indicating possible induction of an apoptotic pathway by RA in these cells. There was no change in RARα and RARβ levels under any of the conditions tested. Cyclin E, a cell cycle checkpoint regulator that promotes G1-S transition (Wimmel et al., 1994) was down-regulated in CRABP2-depleted cells (Fig. 6A). Cyclin E down-regulation is in keeping with the reduced proliferation and increased proportion of cells in the S and G2 phases observed in CRABP2-depleted U251 cells.

Importantly, we found that levels of CRYAB were reduced by ~4 to 5-fold in CRABP2-depleted cells (Fig. 6A). CRYAB is a small heat shock protein associated with apoptosis resistance in MG cells (Goplen et al., 2010; Lee et al., 2012). CRYAB has been shown to directly interact with p53

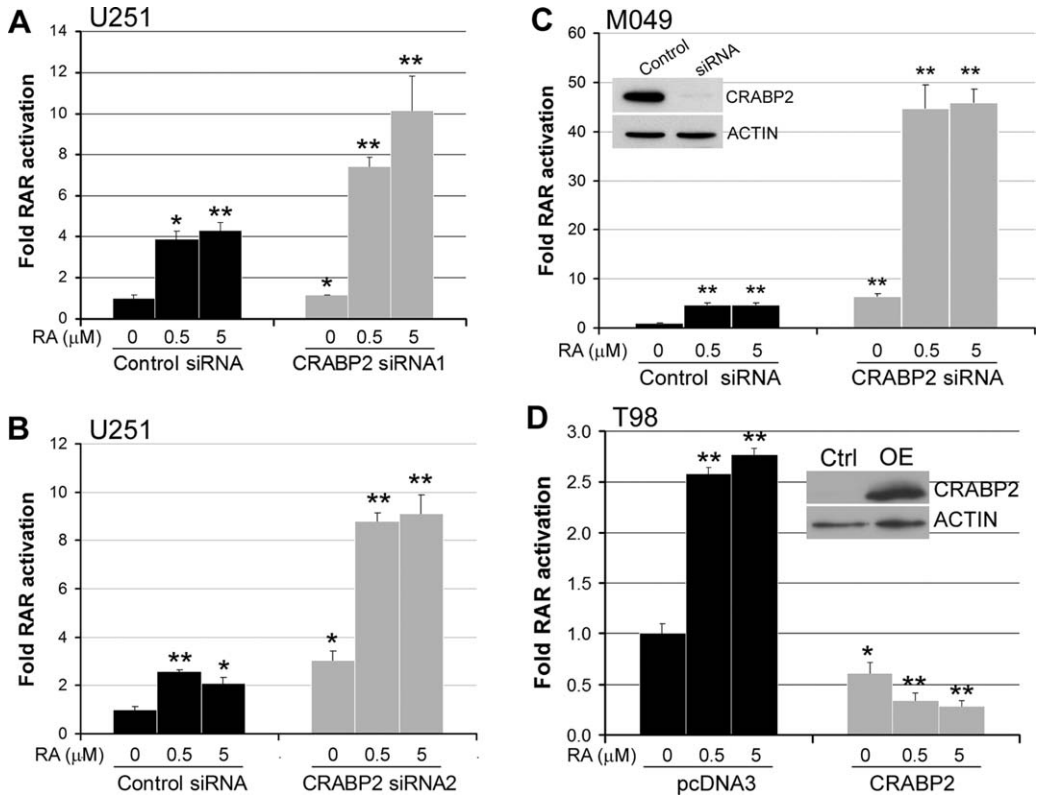

FIGURE 5: CRABP2 inhibits RA-induced RAR activation in MG cells. (A-B) Dose-dependent activation of RAR by RA in U251 cells after CRABP2 depletion using two different CRABP2 siRNAs that target distinct regions of the *CRABP2* RNA. Cells were transfected with a luciferase reporter vector driven by retinoic acid response element (RARE) and cultured in the presence of different amounts of RA as indicated. Luciferase activity (an indication of RAR activation) was corrected for protein concentration in each lysate and is shown as fold relative to control cells transfected with scrambled siRNAs cultured in the absence of RA. (C) CRABP2 was depleted by siRNA transfection in M049 cells (left corner insert). CRABP2-depleted cells showed greatly enhanced RA-induced luciferase activity. (D) T98 cells were co-transfected with a RARE-driven luciferase construct (pGL3-RARE-Luciferase) and a CRABP2 expression construct (pcDNA3-CRABP2) and treated with increasing amounts of RA as indicated. RA-induced increase in luciferase activity was suppressed by CRABP2 overexpression. Western blot analysis of CRABP2 in T98 cells is shown in the right corner. "*" denotes $p < 0.05$, "" $p < 0.01$.**

and caspase 3 to repress their apoptotic function (Liu et al., 2007; Shin et al., 2009). Similar to CRYAB, GFAP levels were reduced by ~6 to 7-fold in CRABP2-depleted cells compared to control cells. GFAP is an intermediate filament protein that is normally expressed in differentiated astrocytes as well as in astrocytoma tumors (Brehar et al., 2015; Choi et al., 2009). GFAP physically associates with CRYAB in astrocytomas cells (Wisniewski and Goldman 1998). The expression of the neural stem cell/radial glial cells marker FABP7 (Feng et al., 1994; Gomez-Lopez et al., 2011; Li et al., 2008), which is also expressed in neurospheres derived from GBM patients and which is associated with MG cell migration (De Rosa et al., 2012; Liang et al., 2005; Mita et al., 2007), was not significantly affected by RA in control cells, with a slight decrease in FABP7 levels observed upon RA treatment in CRABP2-depleted cells.

The possibility of crosstalk between CRABP2 and CRYAB in mediating RA signaling to RARs was examined by co-transfecting a CRYAB expression construct, along with the RARE-driven luciferase reporter, in CRABP2-depleted U251 cells. As previously observed, there was a significant increase in luciferase activity in CRABP2-depleted cells in either the absence or presence of RA. However, this increase in luciferase activity was mitigated by restoration of CRYAB expression, especially in the absence of RA (Fig. 6B). As shown in Fig. 6A, there was an increase in CRYAB upon RA treatment in CRABP2-depleted cells. This increase in endogenous CRYAB levels may explain the relatively small effect of CRYAB restoration on RAR activation in the presence of RA in CRABP2-depleted cells. These results suggest that the roles of CRABP2 (promoting cell survival and attenuating RA signaling) in GBM cells are at least partially mediated through modulation of CRYAB.

Both CRYAB and GFAP are induced in reactive astrocytes under various pathological conditions (Hol and Pekny 2015; Renkawek et al., 1994), with both proteins co-localizing to intermediate filaments in astrocytoma cells (Goplen et al., 2010). As the levels of CRYAB and GFAP are similarly reduced upon CRABP2 depletion in U251 cells, we investigated the possibility of a similar correlation in GBM tumor tissues and other MG cell lines. Analysis of *CRYAB* and *GFAP* RNA levels

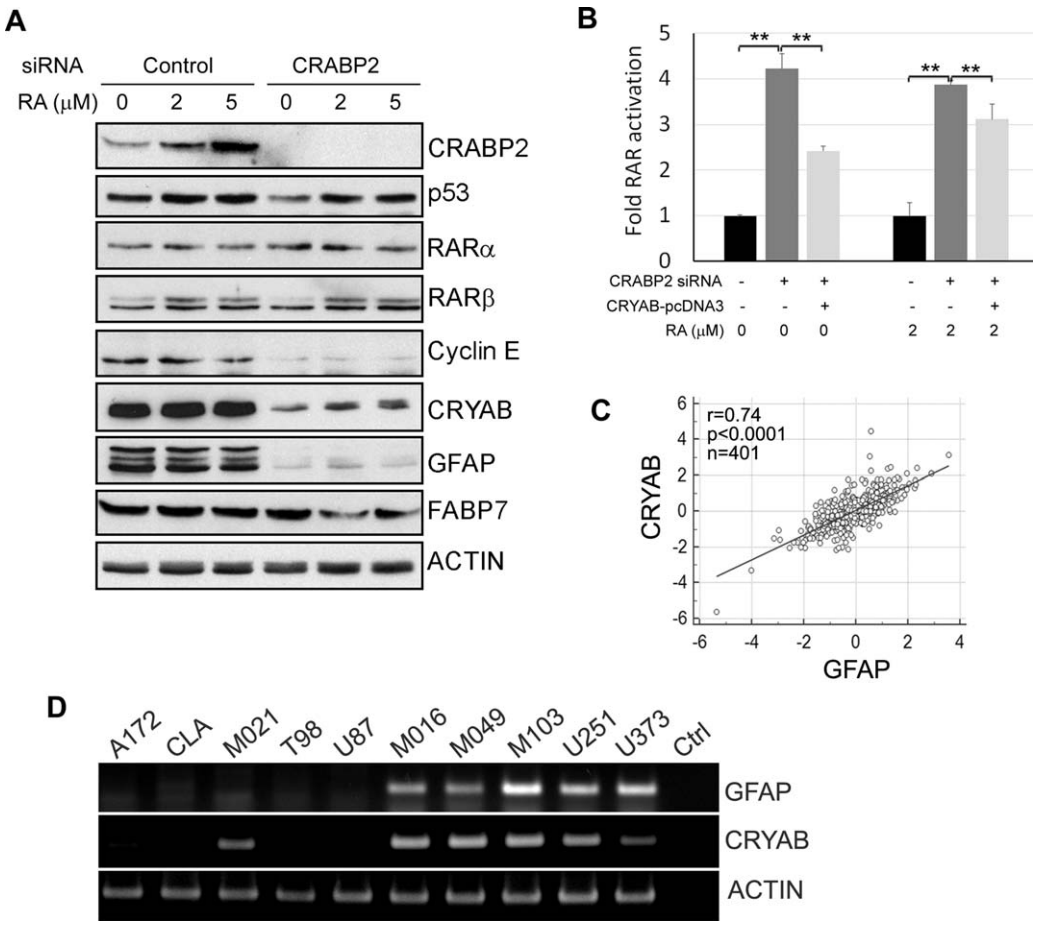

FIGURE 6: CRABP2 depletion affects levels of proteins involved in cellular response to RA. (A) Western blot analysis of U251 cells transfected with CRABP2 siRNA and treated with the indicated concentrations of RA. The antibodies used for the analysis are indicated on the side. β-actin served as the protein loading control for these experiments. (B) The effect of CRYAB on luciferase activity (RAR activation) in CRABP2-depleted cells was measured by co-transfecting U251 cells with pGL3-RARE-luciferase and pcDNA3-CRYAB following CRABP2 depletion. Luciferase activity was then measured in the presence or absence of RA. "" denotes $p < 0.01$. (C) Correlation of *CRYAB* and *GFAP* mRNA levels in a 401-patient GBM cohort obtained from cBioportal network. r denotes correlation coefficient, n, sample size. (D) *CRYAB* and *GFAP* RNA levels were analysed by semi-quantitative RT-PCR in ten MG cell lines. RT-PCR using β-actin primers served as input control for template cDNA. A RT- PCR reaction lacking the cDNA template served as an amplification negative control (Ctrl).**

in a TCGA microarray dataset consisting of GBM tissue from 401 patients revealed a robust and significant correlation ($r = 0.74$, $P < 0.0001$) (Fig. 6C). A similar correlation was also observed in 10 GBM cell lines, with 5/5 GFAP-positive MG cell lines expressing CRYAB, and only 1/5 GFAP-negative MG cell line expressing CRYAB (Fig. 6D). CRYAB and GFAP may therefore be co-induced and/or play synergistic roles under certain pathological conditions (e.g., GBM tumor formation/progression or reactive gliosis). These data provide further support for CRYAB and GFAP functioning as downstream effectors of CRABP2 in GBM cells.

Discussion

Different RA binding proteins, serving as intracellular transporters for RA, play critical and distinct roles in modulating the intracellular trafficking of RA and its biological action. CRABP2 has previously been shown to channel RA to the nucleus for RAR activation (Budhu and Noy, 2002; Dong et al., 1999). Notably, it has been reported that sensitivity of breast cancer cells to RA is controlled by two RA binding proteins, FABP5 and CRABP2, through distinct pathways: FABP5 delivers RA to PPARβ/δ, resulting in increased cell proliferation/survival, whereas CRABP2 transports RA to RARs, inhibiting cell growth (Schug et al., 2007). Thus, resistance to RA action in breast cancer cells can be overcome by reducing the ratio of FABP5:CRABP2 to divert RA from PPARβ/δ to RAR (Schug et al., 2008). Yet a third RA binding protein, CRABP1, has recently been shown to increase RA resistance in breast cancer cells by sequestering RA in the cytoplasm (Liu et al., 2015).

In contrast to other cancers, GBMs express elevated levels of RA signaling molecules (e.g. ALDH1A1, CRBP1, RARs, RXRs) and have elevated levels of retinoids, yet GBM

tumors are highly resistant to the growth-controlling effects of RA (Campos et al., 2011, 2015). The ratio of FABP5 to CRABP2 transcripts is even lower in GBM cells than in normal astrocytes, suggesting that RA resistance in GBM cells is not caused by PPARβ activation (Campos et al., 2015). Accordingly, the relative levels of FABP5:CRABP2 are neither related to tumor grade nor implicated for RA sensitivity in GBM (Xia et al., 2015). Our results indicate that CRABP2 plays an unconventional role in GBM tumors. Specifically, we show that CRABP2 accumulates in the cytoplasm of GBM tumor cells, thereby promoting cell survival, attenuating the transcriptional activity of RAR and inhibiting RA-induced apoptosis by upregulating an anti-apoptotic pathway. Thus, our findings help explain why overall CRABP2 (or relative CRABP2 and FABP5 levels), fail to predict RA response in certain cancers, including GBM (Campos et al., 2011, 2015; Chen et al., 2012; Xia et al., 2015).

Campos et al. (2011) showed absence of CRABP2 in the nucleus of ∼70% of GBM tumors compared to ∼50% of grades II and III astrocytomas, suggesting a trend towards reduced nuclear CRABP2 levels with increasing malignancy. These authors also showed that the levels of proteins favoring cellular RA availability (CRBP1, ALDH1A1) were elevated in astrocytoma tumor tissue compared to non-neoplastic brain tissue, with increasing levels associated with increasing tumor malignancy and shorter patient survival, suggesting impaired RA signaling in astrocytomas (Campos et al., 2011). In our study, we found an inverse correlation between cytoplasmic, but not nuclear, CRABP2 levels, and recurrence-free survival, with recurrence considered an end point for GBM patients. Our findings that cytoplasmic CRABP2 predicts decreased recurrence-free survival in GBM patients and that cytoplasmic CRABP2 is a negative mediator of RA signalling in GBM cells suggest a causative role for cytoplasmic CRABP2 in patient recurrence and tumor progression, perhaps mediated through an attenuated physiological response to RA.

It is noteworthy that the cytoplasmic/nuclear distribution of CRABP2 is considerably less skewed towards the cytoplasm in breast cancer compared to GBM tumors (Liu et al., 2015). For example, in ER-positive breast cancers which are typically sensitive to RA, 51% and 91% of cancers showed high levels (scores of 2 and 3) of CRABP2 in the cytoplasm and nucleus, respectively. In ER-negative breast cancers, typically resistant to RA, 39% and 61% of cancers showed high levels in the cytoplasm versus nucleus, respectively (Liu et al., 2015). In comparison, we observed high levels of cytoplasmic and nuclear CRABP2 in 27.2% and 6.8% of the GBM tumors tested, respectively.

Little is known about the biological activity of CRABP2 in the cytoplasm. An obvious role is to sequester RA in the cytoplasm, thus rendering it unavailable for activation of RARs in the nucleus. Cytoplasmic CRABP2 may also target RA to certain metabolizing enzymes such as CYP26, facilitating RA catabolism to yield polar metabolites (Njar et al., 2006). RA catabolism is believed to be one of the key players in cellular resistance to RA (Njar et al., 2006; Petty et al., 2005; Sessler and Noy, 2005). While we show that CRABP2 accumulates in the cytoplasm in a RA dose-dependent manner in MG cell lines, it remains to be determined whether CRABP2 simply sequesters RA or transports RA to specific sites in the cytoplasm for catabolism. As a third possibility, RA-bound cytoplasmic CRABP2 may activate the extracellular signal regulated kinase 1/2 (ERK1/2), as previously demonstrated for CRABP1, thereby affecting cell cycle progression, cell proliferation and stemness (Persaud et al., 2013). Yet another possibility is that cytoplasmic CRABP2 may directly bind to the RNA-binding protein HuR, thereby enhancing its interaction with target RNAs, leading to their increased stability and expression (Vreeland et al., 2014a). Our discovery that CRABP2 is primarily found in the cytoplasm of GBM cells warrants further studies to examine its exact mechanism(s) of action in these tumors.

CRYAB (αB-crystallin) belongs to an evolutionarily conserved family of small heat shock proteins that function as cytoprotective chaperones (Horwitz, 1992). Induction of CRYAB under various stress conditions confers protection against apoptotic stimuli in different cancer cells (Arrigo et al., 2007). CRYAB is upregulated in MG cells (Goplen et al., 2010; Odreman et al., 2005), and its silencing sensitizes these cells to different apoptotic inducers (Goplen et al., 2010; Lee et al., 2012). In this study, we demonstrate that CRABP2 knockdown sensitizes MG cells to RA-induced RAR activation, with concomitant downregulation of CRYAB. We speculate that CRABP2 may contribute to RA resistance in MG cells through upregulation of CRYAB, which then acts as an inhibitor of RA-induced apoptosis.

GFAP, normally expressed in astrocytes, is up-regulated in reactive astrocytes and serves as a marker for astrocytoma tumors (Brehar et al., 2015; Choi et al., 2009). GFAP levels were markedly reduced upon CRABP2 depletion in MG cells. CRYAB as well as other small heat shock proteins have been shown to interact with GFAP in astrocytes and astrocytoma cells (Goldbaum et al., 2009; Nicholl and Quinlan, 1994; Perng et al., 1999; Wisniewski and Goldman, 1998). This interaction protects the cells against cellular stress. Interestingly, there is a strong correlation between *GFAP* and *CRYAB* RNA levels in GBM tumor tissues as well as MG cell lines, suggesting that these two genes may be co-regulated. Although our study did not address whether *GFAP* and *CRYAB* expression is directly regulated through a CRABP2-dependent mechanism, it does show that reduction of GFAP and CRYAB levels is independent of RA. It is possible that by binding to the RNA-binding protein HuR, CRABP2

enhances HuR's interaction with the *CRYAB* and *GFAP* RNAs, leading to their increased stability and translation (Vreeland et al., 2014a).

In summary, we report the intriguing finding that CRABP2 is predominantly localized in the cytoplasm of GBM tumors, and provide evidence that cytoplasmic CRABP2 is a significant prognostic factor associated with shorter survival in GBM patients. We demonstrate that cytoplasmic CRABP2 promotes MG cell survival and attenuates RA-mediated nuclear RAR activity. Our data suggest that CRABP2 triggers an anti-apoptotic or cyto-protective response in MG cells by upregulating CRYAB and GFAP to resist RA signaling and action. This study underlines the importance of determining the subcellular localization of proteins involved in the regulation of RA bioavailability to predict response to RA. We propose that CRABP2 accumulation in the cytoplasm represents a critical factor causing RA resistance in GBM and that reducing CRABP2 levels may enhance the efficacy of RA therapy.

Acknowledgment

Grant sponsor: Canadian Institutes of Health Research; Grant number: 130314.

The authors thank Elizabeth Monckton and Lei Li for technical assistance. They also thank Xuejun Sun, Jingzhou Huang, Gerry Barron, and the Cross Cancer Institute Cell Imaging Facility for their assistance with cell cycle analysis and imaging of GBM tumor tissue and cells.

References

Adam SA, Schnell O, Poschl J, Eigenbrod S, Kretzschmar HA, Tonn JC, Schuller U. 2012. ALDH1A1 is a marker of astrocytic differentiation during brain development and correlates with better survival in glioblastoma patients. Brain Pathology 22:788−797.

Arrigo AP, Simon S, Gibert B, Kretz-Remy C, Nivon M, Czekalla A, Guillet D, Moulin M, Diaz-Latoud C, Vicart P. 2007. Hsp27 (HspB1) and alphaB-crystallin (HspB5) as therapeutic targets. FEBS Lett 581:3665−3674.

Boorjian SA, Milowsky MI, Kaplan J, Albert M, Cobham MV, Coll DM, Mongan NP, Shelton G, Petrylak D, Gudas LJ, Nanus DM. 2007. Phase 1/2 clinical trial of interferon alpha2b and weekly liposome-encapsulated all-trans retinoic acid in patients with advanced renal cell carcinoma. J Immunother 30:655−662.

Brehar FM, Arsene D, Brinduse LA, Gorgan MR. 2015. Immunohistochemical analysis of GFAP-delta and nestin in cerebral astrocytomas. Brain Tumor Pathol 32:90−98.

Brennan CW, Verhaak RG, McKenna A, Campos B, Noushmehr H, Salama SR, Zheng S, Chakravarty D, Sanborn JZ, Berman SH, et al. 2013. The somatic genomic landscape of glioblastoma. Cell 155:462−477.

Brun M, Coles JE, Monckton EA, Glubrecht DD, Bisgrove D, Godbout R. 2009. Nuclear factor I regulates brain fatty acid-binding protein and glial fibrillary acidic protein gene expression in malignant glioma cell lines. J Mol Biol 391:282–300.

Budhu AS, Noy N. 2002. Direct channeling of retinoic acid between cellular retinoic acid-binding protein II and retinoic acid receptor sensitizes mammary carcinoma cells to retinoic acid-induced growth arrest. Mol Cell Biol 22: 2632−2641.

Campos B, Centner FS, Bermejo JL, Ali R, Dorsch K, Wan F, Felsberg J, Ahmadi R, Grabe N, Reifenberger G, et al. 2011. Aberrant expression of retinoic acid signaling molecules influences patient survival in astrocytic gliomas. Am J Pathol 178:1953−1964.

Campos B, Wan F, Farhadi M, Ernst A, Zeppernick F, Tagscherer KE, Ahmadi R, Lohr J, Dictus C, Gdynia G, et al. 2010. Differentiation therapy exerts antitumor effects on stem-like glioma cells. Clinical Cancer Res 16:2715−2728.

Campos B, Weisang S, Osswald F, Ali R, Sedlmeier G, Bageritz J, Mallm JP, Hartmann C, von Deimling A, Popanda O, et al. 2015. Retinoid resistance and multifaceted impairment of retinoic acid synthesis in glioblastoma. Glia 63:1850−1859.

Cerami E, Gao J, Dogrusoz U, Gross BE, Sumer SO, Aksoy BA, Jacobsen A, Byrne CJ, Heuer ML, Larsson E, et al. 2012. The cBio cancer genomics portal: An open platform for exploring multidimensional cancer genomics data. Cancer Dis 2:401−404.

Chambon P. 1996. A decade of molecular biology of retinoic acid receptors. FASEB J 10:940−954.

Chen NN, Li Y, Wu ML, Liu ZL, Fu YS, Kong QY, Chen XY, Li H, Liu J. 2012. CRABP-II- and FABP5-independent all-trans retinoic acid resistance in COLO 16 human cutaneous squamous cancer cells. Exp Dermatol 21:13−18.

Choi KC, Kwak SE, Kim JE, Sheen SH, Kang TC. 2009. Enhanced glial fibrillary acidic protein-delta expression in human astrocytic tumor. Neurosci Lett 463:182−187.

De Rosa A, Pellegatta S, Rossi M, Tunici P, Magnoni L, Speranza MC, Malusa F, Miragliotta V, Mori E, Finocchiaro G, et al. 2012. A radial glia gene marker, fatty acid binding protein 7 (FABP7), is involved in proliferation and invasion of glioblastoma cells. PloS One 7:e52113.

Dong D, Ruuska SE, Levinthal DJ, Noy N. 1999. Distinct roles for cellular retinoic acid-binding proteins I and II in regulating signaling by retinoic acid. J Biol Chem 274:23695−23698.

Donovan M, Olofsson B, Gustafson AL, Dencker L, Eriksson U. 1995. The cellular retinoic acid binding proteins. J Steroid Biochem Mol Biol 53:459−465.

Duester G. 2008. Retinoic acid synthesis and signaling during early organogenesis. Cell 134:921−931.

Esteller M, Guo M, Moreno V, Peinado MA, Capella G, Galm O, Baylin SB, Herman JG. 2002. Hypermethylation-associated inactivation of the cellular retinol-binding-protein 1 gene in human cancer. Cancer Res 62:5902−5905.

Feng L, Hatten ME, Heintz N. 1994. Brain lipid-binding protein (BLBP): A novel signaling system in the developing mammalian CNS. Neuron 12:895–908.

Fiorella PD, Napoli JL. 1994. Microsomal retinoic acid metabolism. Effects of cellular retinoic acid-binding protein (type I) and C18-hydroxylation as an initial step. J Biol Chem 269:10538−10544.

Gao J, Aksoy BA, Dogrusoz U, Dresdner G, Gross B, Sumer SO, Sun Y, Jacobsen A, Sinha R, Larsson E, et al. 2013. Integrative analysis of complex cancer genomics and clinical profiles using the cBioPortal. Sci Signal 6:pl1.

Garattini E, Gianni M, Terao M. 2007. Retinoids as differentiating agents in oncology: A network of interactions with intracellular pathways as the basis for rational therapeutic combinations. Curr Pharm Des 13:1375−1400.

Godbout R, Bisgrove DA, Shkolny D, Day RS III. 1998. Correlation of B-FABP and GFAP expression in malignant glioma. Oncogene 16:1955−1962.

Godbout R, Miyakoshi J, Dobler KD, Andison R, Matsuo K, Allalunis-Turner MJ, Takebe H, Day RS, 3rd 1992. Lack of expression of tumor-suppressor genes in human malignant glioma cell lines. Oncogene 7:1879−1884.

Goldbaum O, Riedel M, Stahnke T, Richter-Landsberg C. 2009. The small heat shock protein HSP25 protects astrocytes against stress induced by proteasomal inhibition. Glia 57:1566−1577.

Gomez-Lopez S, Wiskow O, Favaro R, Nicolis SK, Price DJ, Pollard SM, Smith A. 2011. Sox2 and Pax6 maintain the proliferative and developmental potential of gliogenic neural stem cells In vitro. Glia 59:1588−1599.

Goplen D, Bougnaud S, Rajcevic U, Boe SO, Skaftnesmo KO, Voges J, Enger PO, Wang J, Tysnes BB, Laerum OD, et al. 2010. alphaB-crystallin is elevated in highly infiltrative apoptosis-resistant glioblastoma cells. Am J Pathol 177: 1618–1628.

Gudas LJ. 1992. Retinoids, retinoid-responsive genes, cell differentiation, and cancer. Cell Growth Differ 3:655–662.

Gudas LJ. 1994. Retinoids and vertebrate development. J Biol Chem 269: 15399–15402.

Gudas LJ, Wagner JA. 2011. Retinoids regulate stem cell differentiation. J Cell Physiol 226:322–330.

Hol EM, Pekny M. 2015. Glial fibrillary acidic protein (GFAP) and the astrocyte intermediate filament system in diseases of the central nervous system. Curr Opin Cell Biol 32:121–130.

Horwitz J. 1992. Alpha-crystallin can function as a molecular chaperone. Proc Natl Acad Sci USA 89:10449–10453.

Huang ME, Ye YC, Chen SR, Chai JR, Lu JX, Zhoa L, Gu LJ, Wang ZY. 1988. Use of all-trans retinoic acid in the treatment of acute promyelocytic leukemia. Blood 72:567–572.

Johnson DR, O'Neill BP. 2012. Glioblastoma survival in the United States before and during the temozolomide era. J Neurooncol 107:359–364.

Lee JS, Kim HY, Jeong NY, Lee SY, Yoon YG, Choi YH, Yan C, Chu IS, Koh H, Park HT, et al. 2012. Expression of alphaB-crystallin overrides the anti-apoptotic activity of XIAP. Neuro-Oncology 14:1332–1345.

Li H, Chang YW, Mohan K, Su HW, Ricupero CL, Baridi A, Hart RP, Grumet M. 2008. Activated Notch1 maintains the phenotype of radial glial cells and promotes their adhesion to laminin by upregulating nidogen. Glia 56: 646–658.

Liang Y, Diehn M, Watson N, Bollen AW, Aldape KD, Nicholas MK, Lamborn KR, Berger MS, Botstein D, Brown PO, et al. 2005. Gene expression profiling reveals molecularly and clinically distinct subtypes of glioblastoma multiforme. Proc Natl Acad Sci USA 102:5814–5819.

Liu RZ, Garcia E, Glubrecht DD, Poon HY, Mackey JR, Godbout R. 2015. CRABP1 is associated with a poor prognosis in breast cancer: Adding to the complexity of breast cancer cell response to retinoic acid. Mol Cancer 14: 129.

Liu RZ, Graham K, Glubrecht DD, Germain DR, Mackey JR, Godbout R. 2011. Association of FABP5 expression with poor survival in triple-negative breast cancer: Implication for retinoic acid therapy. Am J Pathol 178:997–1008.

Liu S, Li J, Tao Y, Xiao X. 2007. Small heat shock protein alphaB-crystallin binds to p53 to sequester its translocation to mitochondria during hydrogen peroxide-induced apoptosis. Biochem Biophys Res Commun 354:109–114.

Lotan R. 1996. Retinoids in cancer chemoprevention. FASEB J 10: 1031–1039.

Mangelsdorf DJ. 1994. Vitamin A receptors. Nutr Rev 52:S32-S44.

Means AL, Gudas LJ. 1995. The roles of retinoids in vertebrate development. Annu Rev Biochem 64:201–233.

Mita R, Coles JE, Glubrecht DD, Sung R, Sun X, Godbout R. 2007. B-FABP-expressing radial glial cells: the malignant glioma cell of origin? Neoplasia 9: 734–744.

Mongan NP, Gudas LJ. 2007. Diverse actions of retinoid receptors in cancer prevention and treatment. Differentiation 75:853–870.

Napoli JL. 1996. Biochemical pathways of retinoid transport, metabolism, and signal transduction. Clin Immunol Immunopathol 80:S52-S62.

Nicholl ID, Quinlan RA. 1994. Chaperone activity of alpha-crystallins modulates intermediate filament assembly. EMBO J 13:945–953.

Njar VC, Gediya L, Purushottamachar P, Chopra P, Vasaitis TS, Khandelwal A, Mehta J, Huynh C, Belosay A, Patel J. 2006. Retinoic acid metabolism blocking agents (RAMBAs) for treatment of cancer and dermatological diseases. Bioorg Med Chem 14:4323–4340.

Noy N. 2010. Between death and survival: Retinoic acid in regulation of apoptosis. Annu Rev Nutr 30:201–217.

Odreman F, Vindigni M, Gonzales ML, Niccolini B, Candiano G, Zanotti B, Skrap M, Pizzolitto S, Stanta G, Vindigni A. 2005. Proteomic studies on low- and high-grade human brain astrocytomas. J Proteome Res 4:698–708.

Ostrom QT, Gittleman H, Fulop J, Liu M, Blanda R, Kromer C, Wolinsky Y, Kruchko C, Barnholtz-Sloan JS. 2015. CBTRUS statistical report: Primary brain and central nervous system tumors diagnosed in the United States in 2008-2012. Neuro-Oncology 17:iv1–iv62.

Perng MD, Cairns L, van den IP, Prescott A, Hutcheson AM, Quinlan RA. 1999. Intermediate filament interactions can be altered by HSP27 and alphaB-crystallin. J Cell Sci 112:2099–2112.

Persaud SD, Lin YW, Wu CY, Kagechika H, Wei LN. 2013. Cellular retinoic acid binding protein I mediates rapid non-canonical activation of ERK1/2 by all-trans retinoic acid. Cell Signal 25:19–25.

Petrie K, Zelent A, Waxman S. 2009. Differentiation therapy of acute myeloid leukemia: Past, present and future. Curr Opin Hematol 16:84–91.

Petty WJ, Li N, Biddle A, Bounds R, Nitkin C, Ma Y, Dragnev KH, Freemantle SJ, Dmitrovsky E. 2005. A novel retinoic acid receptor beta isoform and retinoid resistance in lung carcinogenesis. J Natl Cancer Inst 97: 1645–1651.

Recchia F, Lalli A, Lombardo M, De Filippis S, Saggio G, Fabbri F, Rosselli M, Capomolla E, Rea S. 2001. Ifosfamide, cisplatin, and 13-Cis retinoic acid for patients with advanced or recurrent squamous cell carcinoma of the head and neck: A phase I-II study. Cancer 92:814–821.

Renkawek K, Voorter CE, Bosman GJ, van Workum FP, de Jong WW. 1994. Expression of alpha B-crystallin in Alzheimer's disease. Acta Neuropathol 87: 155–160.

Schug TT, Berry DC, Shaw NS, Travis SN, Noy N. 2007. Opposing effects of retinoic acid on cell growth result from alternate activation of two different nuclear receptors. Cell 129:723–733.

Schug TT, Berry DC, Toshkov IA, Cheng L, Nikitin AY, Noy N. 2008. Overcoming retinoic acid-resistance of mammary carcinomas by diverting retinoic acid from PPARbeta/delta to RAR. Proc Natl Acad Sci USA 105: 7546–7551.

Sessler RJ, Noy N. 2005. A ligand-activated nuclear localization signal in cellular retinoic acid binding protein-II. Mol Cell 18:343–353.

Shin DM, Glisson BS, Khuri FR, Clifford JL, Clayman G, Benner SE, Forastiere AA, Ginsberg L, Liu D, Lee JJ, et al. 2002. Phase II and biologic study of interferon alfa, retinoic acid, and cisplatin in advanced squamous skin cancer. J Clin Oncol 20:364–370.

Shin JH, Kim SW, Lim CM, Jeong JY, Piao CS, Lee JK. 2009. alphaB-crystallin suppresses oxidative stress-induced astrocyte apoptosis by inhibiting caspase-3 activation. Neurosci Res 64:355–361.

Singletary SE, Atkinson EN, Hoque A, Sneige N, Sahin AA, Fritsche HA, Jr., Lotan R, Lu T, Hittelman WN, Bevers TB, et al. 2002. Phase II clinical trial of N-(4-Hydroxyphenyl)retinamide and tamoxifen administration before definitive surgery for breast neoplasia. Clin Cancer Res 8:2835–2842.

Sottoriva A, Spiteri I, Piccirillo SG, Touloumis A, Collins VP, Marioni JC, Curtis C, Watts C, Tavare S. 2013. Intratumor heterogeneity in human glioblastoma reflects cancer evolutionary dynamics. Proc Natl Acad Sci USA 110: 4009–4014.

Tan NS, Shaw NS, Vinckenbosch N, Liu P, Yasmin R, Desvergne B, Wahli W, Noy N. 2002. Selective cooperation between fatty acid binding proteins and peroxisome proliferator-activated receptors in regulating transcription. Mol Cell Biol 22:5114–5127.

Tanaka T, De Luca LM. 2009. Therapeutic potential of "rexinoids" in cancer prevention and treatment. Cancer Res 69:4945–4947.

Verma AK, Conrad EA, Boutwell RK. 1982. Differential effects of retinoic acid and 7,8-benzoflavone on the induction of mouse skin tumors by the complete carcinogenesis process and by the initiation-promotion regimen. Cancer Res 42:3519–3525.

Vreeland AC, Levi L, Zhang W, Berry DC, Noy N. 2014a. Cellular retinoic acid-binding protein 2 inhibits tumor growth by two distinct mechanisms. J Biol Chem 289:34065–34073.

Vreeland AC, Yu S, Levi L, de Barros Rossetto D, Noy N. 2014b. Transcript stabilization by the RNA-binding protein HuR is regulated by cellular retinoic acid-binding protein 2. Mol Cell. Biol 34:2135–2146.

Warrell RP, Jr., Frankel SR, Miller WH, Jr., Scheinberg DA, Itri LM, Hittelman WN, Vyas R, Andreeff M, Tafuri A, Jakubowski A, et al. 1991. Differentiation therapy of acute promyelocytic leukemia with tretinoin (all-trans-retinoic acid). N Engl J Med 324:1385–1393.

Williams SJ, Cvetkovic D, Hamilton TC. 2009. Vitamin A metabolism is impaired in human ovarian cancer. Gynecol Oncol 112:637–645.

Wimmel A, Lucibello FC, Sewing A, Adolph S, Muller R. 1994. Inducible acceleration of G1 progression through tetracycline-regulated expression of human cyclin E. Oncogene 9:995–997.

Wisniewski T, Goldman JE. 1998. Alpha B-crystallin is associated with intermediate filaments in astrocytoma cells. Neurochem Res 23:385–392.

Xia SL, Wu ML, Li H, Wang JH, Chen NN, Chen XY, Kong QY, Sun Z, Liu J. 2015. CRABP-II- and FABP5-independent responsiveness of human glioblastoma cells to all-trans retinoic acid. Oncotarget 6: 5889–5902.